389

Origin of hypergolic ignition of N_2H_4/NO_2 mixtures

Yu Daimon*, Hiroshi Terashima**, and Mitsuo Koshi**†

*Japan Aerospace Exploration Agency (JAXA), 2−1−1 Tsukuba, Ibaraki 305−8050, JAPAN

**The University of Tokyo, 7−3−1 Hongo, Bunkyo-ku, Tokyo 113−8656, JAPAN
   Phone : +81−35−841−0355
†Corresponding address : koshi@rocketlab.t.u-tokyo.ac.jp

Abstract

Hydrazine (N_2H_4) has a unique characteristic inducing hypergolic ignition even at very low temperatures with nitrogen dioxide (NO_2). In order to understand the chemical kinetic origin of this hypergolic nature, thermochemical data (heat of formation, specific heat capacity, and entropy) for chemical species relevant to N_2H_4/NO_2 combustion are firstly evaluated on the basis of quantum chemical calculation at the CBS-QB3 level of theory. Then, a preliminary detailed chemical kinetic mechanism for gas-phase combustion of N_2H_4/NO_2 mixtures has been constructed. Kinetic simulations indicated that sequential reactions of $N_2H_m+NO_2$ (m=4,3,2,1), that is, $N_2H_4+NO_2=N_2H_3+HONO$ (1), $N_2H_3+NO_2=N_2H_3NO_2=N_2H_2+HONO$ (2), $N_2H_2+NO_2=NNH+HONO$ (3), and $NNH+NO_2=N_2+HONO$ (4), are responsible for the hypergolic ignition at low temperatures. Rate constants of these reactions were estimated based on the transition state theory and unimolecular rate theory. The proposed mechanism can predict low temperature ignition of N_2H_4/NO_2 mixtures. The origin of the low temperature ignition is the reaction sequence of hydrogen abstraction by NO_2 from N_2H_4, $N_2H_4=>N_2H_3=>N_2H_2=>NNH=>N_2$. Large amount of heat is released during this reaction sequence, especially by the reaction (4) which produces N_2, and the resulting temperature rise accelerates the reaction (1), which has a small activation barrier.

Keywords : propellant, hypergolic, hydrazine, combustion, kinetics

1. Introduction

A bipropellant combination frequently used in aerospace vehicles is hydrazine (N_2H_4) as a fuel and nitrogen tetroxide (N_2O_4), in fact the NO_2-N_2O_4 equilibrium mixture, as an oxidizer. This combination is known to be hypergolic around room temperature and has been extensively studied experimentally[1)−7)]. However, chemical kinetics of N_2H_4/NO_2-N_2O_4 combustion is not well understood, in spite of these experimental studies.

Ignition characteristic of N_2H_4/NO_2-N_2O_4 bipropellant thruster used in aerospace vehicles is known to be very sensitive to operating conditions, and detailed knowledge of chemical kinetics is required for the optimal design of the bipropellant thruster. Previous studies[5)−7)] indicate that the hypergolic initiation of N_2H_4/N_2O_4 system occurs in the gas phase. Therefore, the understanding of gas phase chemical kinetics of this system is very crucial for the improvement of the thruster performance. However, information on chemical kinetics of N_2H_4 combustion is

very limited and only few mechanism are found in the literature.

After the vaporization of N_2O_4 liquid, the equilibrium between N_2O_4 and NO_2 largely exceeds to NO_2. Therefore, the hypergolic ignition could be explained by the gas phase chemical reactions between N_2H_4 and NO_2. In the all of chemical kinetic mechanisms for N_2H_4/NO_2 gas phase combustion proposed previously[8)−10)], the combustion proceeds on the chain reactions initiated by the production of radicals from thermal decomposition of reactants. Since decomposition of reactants could not occur at low temperatures, the mechanism fails to explain the low temperature auto-ignition.

According to the experiments on the gas phase combustion by Sawyer and Glassman[3)], non-chain and direct reactions between N_2H_4 and NO_2, which may be the hydrogen abstraction by NO_2, might play an important role on the auto-ignition of N_2H_4/NO_2 system. However, there has been no available kinetic data on this and its

consecutive reactions, N₂Hₘ+NO₂. Those elementary reactions are not included in the previous mechanism, and can be key reactions to the hypergolic ignition.

In this study, possible reaction pathways between N_2H_4 and NO_2 are explored by using *ab-initio* quantum chemical calculations. Rate constants of the reactions are evaluated on the basis of the transition state theory (TST). Reaction pathways and their rate constants for the consecutive processes are also examined. The reactions of N_2H_3 produced by the hydrogen abstraction are found to proceed via the formation of a stable intermediate (adduct) and rates of these reactions might be pressure dependent. The master equation analysis is also performed to evaluate these rate constants at pressure of 10 atm. Rate constants of further subsequent reactions of $N_2H_2+NO_2$ and N_2H+NO_2 are also evaluated by using TST and VTST (variational transition state theory). Elementary reactions studied are implemented into a chemical kinetic mechanism of N_2H_4 combustion and simulations are performed for examining the hypergolic reaction at low temperature. During these $N_2H_4+NO_2$ reactions, several chemical species which has no thermochemical data are produced. Thermochemical data for those species are also evaluated in the present study.

2. Thermochemistry

Considerable thermochemical data are required as inputs for the modeling of the chemistries of N_2H_4/NO_2 combustion. In the present study, most of the data are taken from the database presented by Brucat and Ruscic[11]. However, some of the thermochemical data for molecules such as $N_2H_3NO_2$, H_2NN, $HNNO$, and NH_2OH are not available in the literature. In addition, the some values for enthalpy of formation are different from other databases[12),13)]. The enthalpies of formation for selected species relevant to N_2H_4/NO_2 reactions have been obtained by applying the ARM-1 method (Traditional Atomization Reaction Method) proposed by Astryan et al.[14)] in this study.

In the ARM-1, the atomization energy of a molecule M, $\Sigma D_0(M)$, is given by a following equation:

$$\Sigma D_0(M) = \sum E_0(Theor, A) - E_0(Theor, M) \quad (1)$$

Here, A denotes an atom involved in a molecule M, $E_0(Theor, A)$ and $E_0(Theor, M)$ are theoretical energies of A and M obtained by quantum chemical calculations. The enthalpy of formation, $\Delta H_f^0(M, 298K)$, is estimated as

$$\Delta H_f^0(M, 298K) = \Delta H_f^0(M, 0K) + T_{c,calc}(M) - \sum T_{c,exp}(A) \ (2)$$

$$\Delta H_f^0(M, 0K) = \sum \Delta H_f^0(A, 0K) - \Sigma D_0(M, 0K) \quad (3)$$

where $T_{c,calc}(M) = H^0(M, 298K) - H^0(M, 0K)$ is a theoretical value of the thermal energy content for a molecule M and can be obtained from quantum chemical calculations. The $T_{c,exp}(A) = H^0(A, 298K) - H^0(M, 0K)$ values are the experimental values for the constituent atoms in their reference states. These values are taken from Ref. 14 as follows: $T_{c,exp}(H) = 1.012$, $T_{c,exp}(O) = 1.037$, and $T_{c,exp}(N) = 1.036$ kcal mol⁻¹. Values of

Table 1 Heats of formation at 298 K computed by the ARM−1 with CBS−QB3 energyies (kcal mol⁻¹).

Species	Ref. 12	Ref.11	Ref.13	This Work
N₂H₂	49.83	50.47	50.9	47.96
H₂NN	–	–	–	71.22
N₂H₃	47.95	52.57	36.77	53.86
N₂H₄	22.73	22.67	22.78	23.75
HNO	25.32	25.44	23.79	24.499
HON	60.79	–	–	66.72
HNNO	–	–	–	46.76
HNOH	21.53	–	21.05	21.99
HONO	−18.5	–	−18.31	−20.1
HNOO	56.1	–	–	56.72
HNO₂	−14.1	−18.69	14.15	−12.29
NH₂O	15.84	15.78	–	14.22
NH₂NO	17.84	–	–	17.84
NH₂OH	–	–	–	−11.12
N₂H₃ONO	–	–	–	41.19
N₂H₃NO₂	–	–	–	22.89

enthalpy of formation of atom A at 0K, $\Delta H_f^0(A, 0K)$, are also taken from Ref. 14: 51.63, 58.99, and 112.53 kcal mol⁻¹ for H, O and N atom, respectively. Values of $E_0(Theor, A)$, $E_0(Theor, M)$ and $T_{c,calc}(M)$ are evaluated by quantum chemical calculations at the CBS-QB3 level of theory in the present study. Geometries of each molecules are optimized at the level of B3LYP/6-311++G (3df, 3pd) level of theory and resulting vibrational frequencies and moments of inertia are used to calculate heat capacities, enthalpies, and entropies. These geometries are used as input to CBS-QB3calculations. Resulting enthalpies of formation are listed in table 1 and compared with values of other database[11)−13)].

3. Theoretical calculation of rate constants for N₂Hₘ+NO₂ reactions (m=4,3,2,1)

Search of reaction pathways for the $N_2H_4+NO_2$ and its consecutive reactions have been performed at the B3LYP /6-311++G (3df, 3pd) level of theory. Transition states are extensively searched and if a transition state (TS) was found, IRC (intrinsic reaction coordinate) calculation was conducted in order to assign reactants and products of this TS. Energies of those stationary states were calculated by CBS-QB3 method. All calculations were performed by using GAUSSIAN 03 program suite. Rate constant for the reaction having TS was calculated by using GPOP[15)]. GPOP program suite can also be used for the reaction without TS such as $N_2H_3+NO_2$ on the basis of VTST (variational TST). A master equation analysis for dissociation and chemical activation reactions was performed by using a SSUMES (Steady-State Unimolecular Master-Equation Solver) developed by Miyoshi[16)].

3.1 N₂H₄+NO₂=N₂H₃+HONO (Reaction (1))

This can be the initiation of N_2H_4/NO_2 hypergolic explosion. The reaction is endothermic by 3.98 kcal mol⁻¹

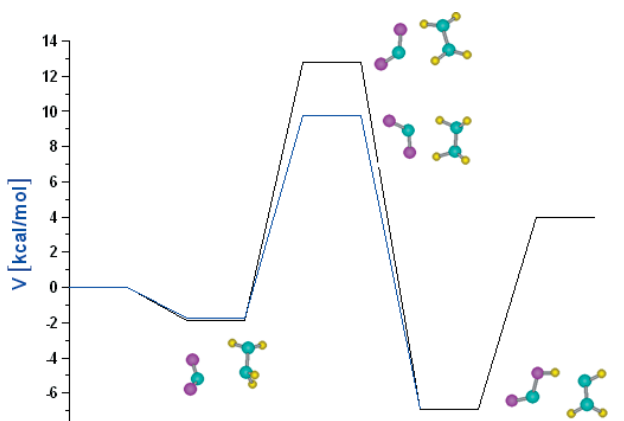**Figure 1**   Energy diagram of $N_2H_4+NO_2$ reactions. (CBS−QB3)

Figure 2   Energy diagram of $N_2H_3+NO_2=N_2H_3NO_2=N_2H_2+$ HONO reactions(CBS−QB3).

(based on CBS-QB3 energy at 0K). Since NO_2 is a radical, relatively low activation barrier is expected. Indeed, two TSs are found with activation barrier of 12.82 (TS1) and 9.77 (TS2) kcal mol^{-1}, respectively. IRC calculations indicate those TSs correlate to stable adducts on both reactant and product side, as shown in Figure 1. Both TS1 and TS2 correlate the same adduct on product side with the energy of −6.92 kcal mol^{-1}. Adducts on reactant side are different from each other for TS1 and TS2, though the energy is very similar (−1.87 and −1.74 kcal mol^{-1} for TS1 and TS2 channels, respectively). The energy diagram is shown in Figire 1.

A simple TST calculation was performed in the present study by neglecting the existence of these adducts. The rate constants are corrected for tunneling by assuming asymmetric Eckart potential[17], but these corrections are negligible because of rather loose TS (imaginary frequencies of 708 and 332 cm^{-1}, for TS1and TS2, respectively). Following modified Arrhenius expressions are obtained.

$$TS\,1 : k = 48.9 \times T^{3.43} \exp(-5566/T)$$
$$TS\,2 : k = 12.0 \times T^{3.23} \exp(-4076/T) \qquad cm^3 mol^{-1} s^{-1}$$

Another TS with the barrier height of 9.27 kcal mol^{-1} was also found, but this TS correlates to different products, $N_2H_3+HNO_2$ which is 12.0 kcal mol^{-1} endothermic. No further study was performed for this pathway because of its higher endothermicity.

3.2 $N_2H_3+NO_2=N_2H_3NO_2=N_2H_2+$HONO (Reaction(2))

N_2H_3 produced by the reaction (1) will further react with NO_2. Since both N_2H_3 and NO_2 are radicals, recombination products are expected to form without any energy barrier. Two isomers, $N_2H_3NO_2$ (ΔH=-35.79 kcal mol^{-1}) and N_2H_3 ONO (ΔH=-17.82 kcal mol^{-1}), are possible for the recombination of N_2H_3 and NO_2. Production of those adducts without energy barrier was confirmed by performing scanning calculations of the potential energy surface. $N_2H_3NO_2$ further decomposes to yield a reduced product (N_2H_2), whereas N_2H_3 ONO will produce an oxidation product (N_2H_3O). A primary concern in the present study is the exothermic process of the initial stage of N_2H_4 reaction, and the fate of $N_2H_3NO_2$ was searched in detail. Investigation of consecutive reactions of N_2H_3 ONO
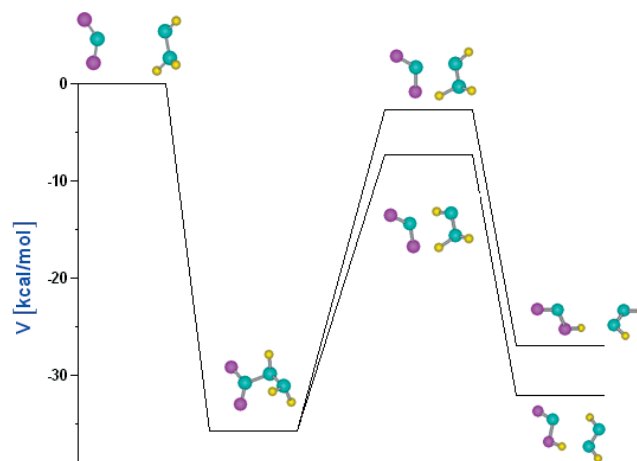
is open for future studies.

Two TSs were found for the decomposition of $N_2H_3NO_2$ to produce N_2H_2 and HONO. One (Channel-1) leads to formation of t-N_2H_2+HONO with a barrier height of 28.46 kcal mol^{-1} (measured from $N_2H_3NO_2$) and another (Channel-2) is a pathway to produce c-N_2H_2+HONO with a barrier height of 33.14 kcal mol^{-1}. Energies of these TSs are below the reactant energy. Energy diagram of these reactions are depicted in Figure 2.

Both channel 1 and 2 are exothermic (ΔH=-32.09 for channel1and ΔH=-27.05 kcal mol^{-1} for channel2), and a master equation analysis is required to evaluate the rate constants of these chemical activation reactions.

At first, the high-pressure limiting rate constant for the recombination of $N_2H_3+NO_2$ was calculated on the basis of VTST method by using the GPOP program suite. The reaction coordinate of the recombination was approximated by a N-N bond length in the O_2N-NHNH$_2$ ($N_2H_3NO_2$) molecule, and partial optimization of the structure at the fixed N-N bond length was performed at the B3LYP /6-311++G (3df, 3pd) level of theory. Vibrational frequencies and principle moments of inertia on each position of reaction coordinate were used to calculate the micro-canonical rate constant, k(E), for the recombination reaction of $N_2H_3+NO_2$. Resulting VTST rate constant (which is the high-pressure limiting rate constant) is shown in Figure 3 as the 'Total rate constant'. Rate constants of the chemical activation reactions for each of three channels, (channels 1, 2 and recombination channel of $N_2H_3+NO_2=N_2H_3NO_2$) were calculated at p=10 atm by using SSUMES program suite. Results are also depicted in Figure 3.

Rate constants for the unimolecular dissociation of $N_2H_3NO_2$ were also calculated at p=10 atm for the three channels using SSUMES and results are depicted in Figure 4.

Large deviations from high-pressure limiting rate constants at high temperatures are evident in this figure and these are caused by non-equilibrium distributions of internal energy even at p=10 atm. It is noted that such non-equilibrium effect i.e., deviation from high-pressure rate constant, is more notable for the pathway with higher
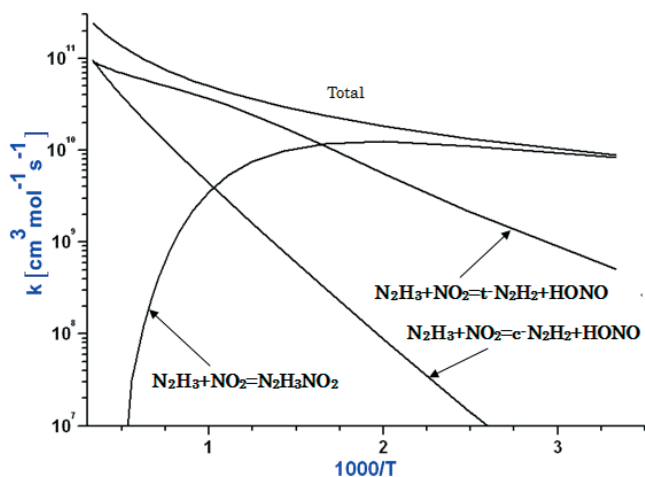
Figure 3 Rate constants for the chemical activation reaction of $N_2H_3+NO_2$. The 'Total' rate constant is the high-pressure limiting rate constant calculated by VTST. Other three rate constants are obtained by solving master equations at p=10 atm.
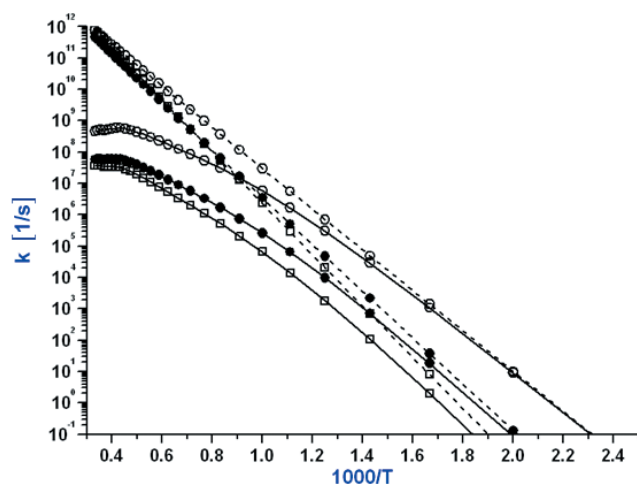

Figure 4 Rate constants of unimolecular dissociation of N_2H_3 NO_2. Broken lines are for high-pressure limiting rate constants, solid curves are calculated at p=10 atm. Open circles : $N_2H_3NO_2$=t-N_2H_2+HONO, open squres : $N_2H_3NO_2$=c-N_2H_2+HONO, closed circles : $N_2H_3NO_2$=N_2H_3+NO_2.

energy barrier.

3.3 $N_2H_2+NO_2$=NNH+HONO (Reaction (3))

Both t-N_2H_2(trans) and c-N_2H_2(cis) can be produced by the reaction (2), as shown in Figure 2, but the production rate of t-N_2H_2 is much faster because of the lower energy barrier height. In the present study, t-N_2H_2+NO_2 reaction was implemented in the modified chemical kinetic mechanism. Adducts with shallow potential minima were found both reactant and product paths. The TS has Cs symmetry with its barrier height of 11.88 kcal mol^{-1}. The imaginary frequency of this TS is 1509 cm^{-1} and the tunneling effect might be important at lower temperatures. The rate constant obtained with Eckart tunneling correction is as follow.

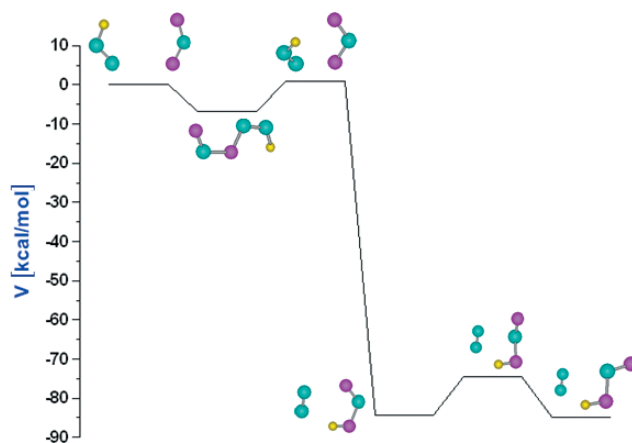$$k = 1.12x10^{-3}T^{4.47}\exp(-3615/T) \text{ cm}^3\text{mol}^{-1}\text{s}^{-1}$$

Figure 5 Energy diagram of NNH+NO_2=N_2+HONO reaction. (CBS−QB3)

3.4 NNH+NO_2=N_2+HONO (Reaction(4))

This reaction has very large exothermicity (ΔH=-84.76 kcal mol^{-1}) because of the production of N_2. A TS with very low activation barrier (1.93 kcal mol^{-1}) was found. The IRC calculation indicated that products of this reaction were N_2 and cis form of HONO, c-HONO, as shown in Figure 5.

TST calculation results in the following rate constant.

$$k = 17.35xT^{2.84}\exp(-842/T) \text{ cm}^3\text{mol}^{-1}\text{s}^{-1}$$

t-HONO is slightly stable than c-HONO, but the difference (0.43 kcal mol^{-1}) is small. The barrier height of the isomerization reaction from t-HONO to c-HONO was found to be 10.36 kcal mol^{-1}. It is expected that c-HONO produced by the this reaction has large excess internal energy because of large exothermicity of the reaction. Therefore, c-HONO produced is readily converted to t-HONO.

4. Kinetic simulation of auto-ignition

A chemical kinetic mechanism for the N_2H_4/NO_2 combustion has been developed by modifying the mechanism originally proposed by Ohminami et al.[9), 10]. The modified mechanism (hereafter, mechanism A) consists of 33 species and 239 reactions. Most of elementary reactions for N-H species and their rate constants in the mechanism were taken from Dean and Bozzelli[12]. The subset of H_2 combustion in the mechanism of Ohminami is replaced by a recent mechanism proposed by an author[18], which is appropriate for high-pressure conditions. It is noted that some of the rate constants for the pressure dependent reactions in Ref. 12 are only given at p=0.1, 1 and 10 atm. Those reactions include dissociation of N_2H_4, N_2H_3, and N_2H_2, isomerization of N_2H_2 (HNNH) to H_2NN, and chemical activation reactions of NH_2+NH_2=N_2 H_3+H, NH_2+NH_2=H_2NN+H_2. In the present study, a target pressure is fixed to p=10 atm, and values of these rate constants in Ref.12 are used. The ignition delay times obtained with the mechanism A are displayed in Figure 6 (broken line).

As can be seen, the delay time at T=800K is over 10 s and it is found that no ignition is possible below 800K.

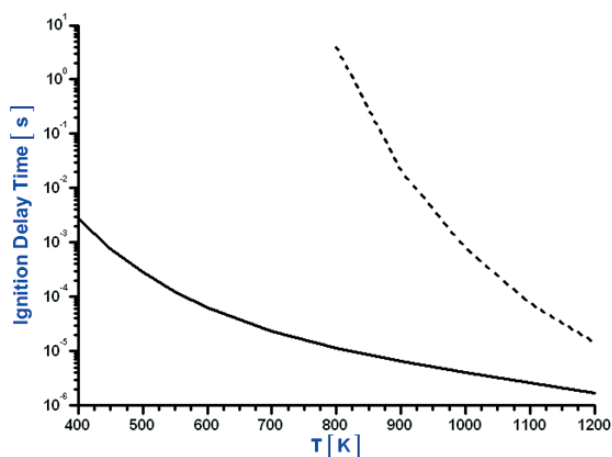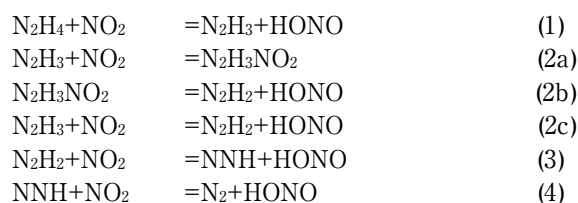Reactions of N_2H_4+NO_2 and subsequent reactions

Figure 6 Ignition delay times of $N_2H_4/NO_2=3/1$ mixture at p= 10 atm. Broken line : mechanism A, Solid line : mechanism B.

described in the previous sections are implemented into the mechanism A. This modified mechanism (mechanism B) includes the following elementary reactions.

$$N_2H_4+NO_2 \quad =N_2H_3+HONO \quad (1)$$
$$N_2H_3+NO_2 \quad =N_2H_3NO_2 \quad (2a)$$
$$N_2H_3NO_2 \quad =N_2H_2+HONO \quad (2b)$$
$$N_2H_3+NO_2 \quad =N_2H_2+HONO \quad (2c)$$
$$N_2H_2+NO_2 \quad =NNH+HONO \quad (3)$$
$$NNH+NO_2 \quad =N_2+HONO \quad (4)$$

Isomers of N_2H_2 and HONO (trans and cis) are not distinguished in the mechanism B and rate constants of reactions (2a), (2b), and (2c) are only given at p=10 atm. Ignition delay times of a $N_2H_4/NO_2=3/1$ mixture at p=10 atm were calculated for the adiabatic combustion (with constant enthalpy and pressure). Results are depicted in Figure 6. The ignition delay times were defined as the time required for the 100 K temperature increase. As can be seen in the figure, the ignition delay times calculated by the mechanism A is much longer than those obtained by the mechanism B. The ignition delay times obtained with the mechanism A below 800 K are longer than 10 second, and practically no ignition is possible. On the other hand, the mechanism B gives the ignition delay time of 2.8 ms at 400 K. This indicates that the reactions of (1)-(4) play an essential role for the hypergolic ignition of N_2H_4 at low temperatures.

5. Concluding remarks

For the understanding of the chemical kinetic origin of the hypergolic ignition of N_2H_4/NO_2 mixture, a preliminary mechanism was constructed. The proposed mechanism can predict possible ignition of N_2H_4/NO_2 even at room temperature. The origin of the low temperature ignition is the reaction sequence of hydrogen abstraction by NO_2 from N_2H_4, $N_2H_4=>N_2H_3=>N_2H_2=>NNH=>N_2$. Large amount of heat is released during this reaction sequence,

and the resulting temperature rise accelerates the reaction (1), which has a small activation barrier.

Although the proposed mechanism successfully predicts the hypergolic ignition of N_2H_4/NO_2 reaction system, the present mechanism is still 'preliminary'. Following problems remain to be solved.

1) Calculations of the rate constants for chemical activation and unimolecular reaction are required at wide range of pressures to obtain the complete mapping of $k(T,P)$.

2) Production of NH_3 ONO and its consecutive reactions have to be considered. Those reactions could be important for the oxidation pathways of N_2H_4.

3) Reactions of isomers of N_2H_2 and HONO have to be included, though the importance of those reactions is not clear.

References

1) B. R. Lawver, AIAA J., 4, 659−662 (1966).
2) A. B. Ray, G. Koehler, G. E. Salser, L. Dauerman, AIAA J., 6, 2186−2187 (1967).
3) R. F. Sawyer, I. Glassman, Proc. Combust. Inst., 11, 861−869 (1967).
4) M. A. Saad, M. B. Detweiler, M. Sweeney, AIAA J., 8, 1073−1078 (1972).
5) W. Daimon, M. Tanaka, I. Kimura, Proc. Combust. Inst., 20, 2065−2071 (1984).
6) M. Tanaka, W. Daimon, I. Kimura, J. Propulsion Power, 1, 314−316 (1984).
7) W. Daimon, Y. Goto, I. Kimura, J. Propulsion Power, 7, 946−952 (1991).
8) L. Catoire, J. Luche, G. Dupre, C. Paillard, Shock Waves, 11, 97−103 (2001).
9) K. Ohminami, H. Ogawa, A. K. Hayashi, Sci. Tech. Energetic Materials, 69, 1−7 (2008) (in Japanese).
10) K. Ohminami, S. Sawai, T. K. Uesugi, N. Yamanishi, M. Koshi, 45th AIAA/ ASME/SAE/ASEE Joint Propulsion Conference & Exhibit., AIAA−2009−5044 (2009).
11) A. Brucat, B. Ruscic, "Third millennium ideal gas and condensed phase thermochemical database for combustion with updates from active thermochemical tables", ANL−05 /20, TAE960 (2005).
12) A. M. Dean, J. W. Bozzelli, "Combustion chemistry of nitrogen", in Gas Phase Combustion Chemistry, ed. by Gardiner, W.C.Jr., Springer-Verlag, New-York (2000).
13) R. J. Kee, F. M. Rupley, J. A. Miller, "The Chemkin thermodynamic data base", Sandia National Laboraatories Report SAND87−8215B (1987).
14) R. Astryan, J. W. Bozzelli, and J. M. Simmie, J. Phys. Chem., A112, 3172−3185 (2008).
15) A. Miyoshi, http://www.frad.t.u-tokyo.ac.jp/ miyoshi/ gpop/ (accessed : 16-November 2011) (online)
16) A. Miyoshi, http://www.frad.t.u-tokyo.ac.jp/ miyoshi/ ssumes/ (accessed : 16-November 2011) (online)
17) B. C. Garrett and D. G. Truhlar, J. Phys. Chem., 83, 2921−2926 (1979).
18) K. Shimizu, A. Hibi, M. Koshi, Y. Morii, N. Tsuboi, J. Propulsion Power 27, 383−395 (2011).

N₂H₄／NO₂混合気の自己着火特性の起源

大門優*，寺島洋史**，越光男***†

　N₂H₄-N₂O₄混合系は室温付近でも自発着火するが，その化学反応機構は不明である。本研究では，N₂H₄-N₂O₄の低温での自発着火を説明できる詳細化学反応機構を構築し，この系の燃焼特性を予測した。詳細化学反応機構を構築するためには，まずその系に含まれるラジカルや反応中間体の生成熱，比熱などの熱力学データが必要となるが，N₂H₄-N₂O₄反応系に含まれる化学種の熱力学データの多くについて実験値が存在せず，反応機構を構築するためにはまずこれらの熱力学データをそろえる必要がある。本研究では，まず量子化学計算と統計熱力学に基づいてこれらの熱力学データの推算を行った。ついで，N₂H₄／NO₂反応系で重要な素反応について，量子化学計算によりポテンシャルエネルギー局面を計算し，遷移状態理論および単分子反応論に基づいて各素反応の速度定数を求めた。これらの素反応を含む詳細反応機構を構築し，着火シミュレーションを行った。構築した反応機構により低温における自己着火を説明することができた。低温での自着火は，N₂H₄からのNO₂による逐次的な水素引き抜き反応によるN₂の生成と，N₂生成による熱的なフィードバック機構により起こることを明らかにした。

*宇宙航空研究開発機構　〒305-8050　茨城県つくば市2-1-1

**東京大学工学系研究科総合研究機構　〒113-8656　東京都文京区本郷7-3-1
Phone：+81-35-841-0355
†Corresponding address：koshi@rocketlab.t.u-tokyo.ac.jp